

Article

Genetic Mapping and Identification of the Gibberellin 3-Oxidase Gene *GA3ox* Leading to a GA-Deficient Dwarf Phenotype in Pumpkin (*Cucurbita moschata* D.)

Ziyang Min ^{1,2}, Xinjun Hu ², Xiaoxia Han ², Yongqi Li ², Jiajia Li ², Duanhua Wang ², Longjun Sun ¹ and Xiaowu Sun ^{1,*}

¹ Department of Horticulture, Hunan Agricultural University, Changsha 410128, China; minziyang1220@163.com (Z.M.); longjun.sun@hotmail.com (L.S.)

² Department of Vegetable Research Institute, Hunan Academy of Agricultural Sciences, Changsha 410125, China; huxinjun1970@163.com (X.H.); xiaoxiahanhan@163.com (X.H.); cslyqdf3@163.com (Y.L.); jjagh1011@163.com (J.L.); duanhuawang0559@163.com (D.W.)

* Correspondence: sunxiaowu2007@126.com

Abstract: Plant height is an important indicator in the ideal plant model and contributes to optimizing yield and lodging resistance. The emergence of a dwarfing phenotype provides an opportunity for plant height improvement. In a previous study, we identified a dwarf mutant Si1 in pumpkin (*Cucurbita moschata* D.) obtained by ethyl methane sulfonate (EMS) mutagenesis of the inbred line N87. Phenotype identification for Si1 revealed a decrease in cell size and shorter internodes than those of wild type. Genetic analysis revealed that the dwarf mutant trait was controlled by a single recessive gene, *CmaSI1*. By bulked segregant analysis (BSA) and subsequent fine mapping, we mapped the *CmaSI1* locus to a 463 kb region on chromosome 8 that contained 28 annotated genes in the F₂ population. Only one nonsynonymous single nucleotide polymorphism (SNP) in *CmoCh08G006170* was obtained according to whole-genome resequencing of the two parents. *CmoCh08G006170*, a homolog of Arabidopsis gibberellin 3-beta hydroxylase (*GA3ox*), is a key enzyme in the regulation of bioactive gibberellins (GAs). RNA-seq analysis and qRT-PCR showed that the expression level of *CmoCh08G006170* in stems of Si1 was changed compared with that of wild type. The dwarf phenotype could be restored by exogenous GA₃ treatment, suggesting that Si1 is a GA-deficient mutant. The above results demonstrated that *CmoCh08G006170* may be the candidate gene controlling the dwarf phenotype. This study provides an important theoretical basis for the genetic regulation of vine length and crop breeding in pumpkin.



Citation: Min, Z.; Hu, X.; Han, X.; Li, Y.; Li, J.; Wang, D.; Sun, L.; Sun, X. Genetic Mapping and Identification of the Gibberellin 3-Oxidase Gene *GA3ox* Leading to a GA-Deficient Dwarf Phenotype in Pumpkin (*Cucurbita moschata* D.). *Agronomy* **2022**, *12*, 1779. <https://doi.org/10.3390/agronomy12081779>

Academic Editor: Ali Raza

Received: 12 June 2022

Accepted: 24 July 2022

Published: 28 July 2022

Publisher's Note: MDPI stays neutral with regard to jurisdictional claims in published maps and institutional affiliations.



Copyright: © 2022 by the authors. Licensee MDPI, Basel, Switzerland. This article is an open access article distributed under the terms and conditions of the Creative Commons Attribution (CC BY) license (<https://creativecommons.org/licenses/by/4.0/>).

Keywords: pumpkin; dwarf mutant; BSA; RNA-seq; *GA3ox*

1. Introduction

The ideal plant model has a significant impact on the growth of crops, and plant height is one of the important indicators in the plant model. Moderate dwarfing better optimizes crop yield and prevents lodging resistance, which saves land resources by improving the yield per unit area [1,2]. In the middle of the 20th century, semidwarf rice varieties significantly increased the yield per unit area of rice, which was known as the first “Green Revolution” in the history of rice breeding [3]. Since then, dwarfing and semidwarfing traits have been widely introduced into important crops and have effectively alleviated the trade-off between high yield and easy lodging [4,5]. The breeding and promotion of dwarfing varieties have greatly improved productivity and the progress of human society.

Many dwarfing mutants have been found in important food crops such as maize, wheat, and rice [6,7]. Among them, more than 90 dwarfing genes in rice, 26 in wheat, and 20 in maize were identified by using dwarfing materials, such as *predominant semidwarf1* (*sd1*) [8], *shortened basal internodes* (*SBI*) [9], reduced height genes *Rht-B1b*, *Rht-D1b* and

Rht18 [10,11], and brassinolide biosynthesis inhibitor *BRI1* [12]. Moreover, many studies have indicated that dwarfing genes are involved in the biosynthesis pathways of plant hormones, which are associated with regulating cell elongation and division [13–15]. For gibberellins (GAs), the well-known “Green Revolution” GA20 oxidases and the rice semi-dwarf gene *sd1* result in dwarfing mutants by regulating degraded bioactive GAs [3,8]. Genes involved in BR biosynthesis were found to regulate plant height [16]. In pepper, a novel single base mutation in *CaBRI1* associated with BR insensitivity caused a dwarf mutant [17]. In addition, Multani et al. (2003) indicated that the key IAA delivery genes *ABCB1/PGP1* were associated with a dwarfing phenotype in the maize mutant BR2 and sorghum mutant dwarf3, showing that auxins also play a role in the regulation of the plant height [13].

Cucurbitaceae crops are important vegetable species, and some dwarf varieties have been reported and applied to crop improvements. Dong et al. (2018) reported a dwarfism gene, *Clao10726*, in watermelon by applying next-generation sequencing technology; two SNPs located in the promoter of the gene led to significantly shorter plants [2]. In another case of dwarfism in watermelon, a 13 bp deletion in the *Clao15407* gene, which encodes a gibberellin 3 β -hydroxylase, resulted in a GA-deficient dwarf phenotype [18]. Dwarf mutants such as CP, CP-2, SCP, SI1, and CSDM1 were also discovered in cucumber [19,20], and the completion of cucumber genome sequencing accelerated the identification of cucumber short stem genes [21]. Li et al. (2011) cloned a homolog of the cytokinin oxidase (*CKX*) gene involved in dwarfism in cucumber, and a 3-bp deletion in the first exon led to the loss of gene function and served as a marker for marker-assisted selection of the compact phenotype [22]. A single-base mutation (C-T) located in the cucumber gene *Csa3G872760* that was caused by EMS mutagenesis resulted in a dwarf phenotype in cucumber; this promoter consists of a 39-residue F-box motif followed by 14 putative leucine-rich repeats (LRRs) [20]. The above studies on the location and cloning of dwarfing genes in Cucurbitaceae crops provide a suitable reference for the development of this study.

Pumpkin, an economically important cucurbitaceae crop, is widely cultivated and consumed worldwide due to its high nutritional value [23,24]. According to the length of the main vine, pumpkins can be divided into three types: trailing, semitrailing, and short vine. *Cucurbita pepo* L. is mainly of the short vine and semitrailing types. *Cucurbita maxima* D. is mainly of the semitrailing and trailing types. *Cucurbita moschata* D. is mainly of the vine type. Currently, research on the short vine trait in pumpkin mainly focuses on *C. pepo* and *C. maxima*. There are relatively few studies on the short vine characteristics of *C. moschata* due to limited materials. Wu et al. (2011) constructed the AFLP analysis system for dwarf *C. moschata* and screened 96 polymorphic primers between dwarf and vine inbred lines. It laid a good foundation for tropic pumpkin dwarf vine mapping [25]. With the development of molecular biology, a high-density genetic linkage map of pumpkin was constructed and contributed to enhanced functional research on the pumpkin. Xiang et al. (2018) constructed a saturated EST-SSR genetic map and located three major QTLs for the gibberellin-sensitive dwarf type in *C. pepo*, with a candidate region of 1.39 Mb [26]. Wang et al. (2014) studied the dwarf mutant *dm1* in *C. maxima*, which is controlled by a single recessive gene *DM1*, and the gene was roughly located in an 11.2 kb region by amplified fragment length polymorphism (AFLP) markers [27]. Zhang et al. (2015) identified a candidate gene, *Cma004516*, that encodes a gibberellin-20 oxidase from the *C. maxima* dwarf mutant SQ026; this gene had a 1249-bp deletion in its promoter in bush-type lines, and its expression level was significantly increased [28]. For *C. moschata*, Wu et al. (2008) demonstrated that fifty-eight transcript-derived fragments (TDFs) have been successfully sequenced and identified based on the internode development of a near-isogenic bush mutant of *C. moschata* [29]. This was the first study of gene expression levels in *C. moschata*. The *CmV1* gene, which may be related to vine elongation in *C. moschata*, was identified by DNA-AFLP combined with RACE technology, but no verification has been carried out to date.

In this study, we identified a dwarf mutant Si1 by treating the *C. moschata* inbred line N87 with EMS mutagenesis, and genetic analysis showed that the mutant phenotype was controlled by a single recessive gene. By using BSA-Seq and further mapping, the

candidate gene *CmoCh08G006170*, which encodes a gibberellin 3 β -hydroxylase (*GA3ox*), served as the most likely candidate gene for the dwarf phenotype of Si1. Nonsynonymous single nucleotide polymorphisms (SNPs) were detected, and the expression level of *CmoCh08G006170* in the stem of Si1 was changed compared with the wild type (WT) N87. This study provides new genetic resources and a theoretical basis for understanding the regulatory mechanisms of dwarfism, which is conducive to improving pumpkin breeding.

2. Materials and Methods

2.1. Plant Materials

Si1, the dwarf mutant, was obtained from an EMS mutagenized population of the pumpkin inbred line N87. N87, a high-generation inbred line, was bred by the Hunan Vegetable Research Institute, Changsha, Hunan, China. It demonstrates strong growth, has short gourd-shaped fruit, a sweet taste, and high resistance to powdery mildew and blight in the field [30]. The specific steps of EMS treatment were reported by Min et al. (2021) [31]. The plant materials were grown in the experimental field for observation and sampling. For the genetic analysis of the dwarf mutant genes, different cross combinations were constructed. Si1 (P_2) was crossed with N87 (P_1) to generate an F_1 population, and the F_1 population was self-pollinated to produce F_2 progeny; BC_1P_1 and BC_1P_2 progeny were then generated by BCs of $F_1 \times N87$ and $F_1 \times Si1$, respectively. The dwarf ratios of the F_1 and segregation populations were analyzed by a chi-squared test using SAS software (SAS Institute, Cary, NC, USA, 2001).

2.2. Plant Phenotyping and Morphological Characterization

Pumpkin is an infinitely growing crop, its vines can reach 4–5 m. The first twenty nodes of the main vine were chosen to exhibit plant height in this study; the growth period of pumpkin includes the periods of clustering stage and vine elongation stage. Generally, pumpkins enter the vine elongation period from the sixth node and the length of the internodes tends to stabilize after the eighth node. So we chose the main vine of the eighth node as the internode length measurement object. The main vines containing wild-type and mutant internodes were measured in two places: the eighth node and the first twenty nodes. Other traits were also measured, including leaves and stem diameter. Each indicator was measured as the average of ten plants grown under the same conditions, and three replicates were used for each measurement. The error bars represent the SEs from three independent experiments. The data were analyzed by ANOVA using SAS software in the study. For morphological characterization, the eighth internode was cut into 3-mm pieces and fixed in a formalin-acetic acid-alcohol (FAA) solution (70% alcohol: 3.8% formalin: glacial acetic acid = 18:1:1) for 24 h, dehydrated with a different concentrations of ethanol (75%, 85%, 90%, 95%, and $2 \times 100\%$), infiltrated with 100% xylene and embedded in paraffin. The samples were cut into 10- μ m slices by an RM2016 microtome (Leica, Wetzlar, Germany) and mounted on glass slides. Then, they were stained with 1% toluidine blue for 5 min and washed with deionized water and ethanol. Finally, the sections were observed and imaged using an Olympus BH-2 photomicroscope (Olympus, Tokyo, Japan).

2.3. Bulk Segregant Analysis (BSA)

Leaf samples were collected from 20 randomly selected normal-vine individuals and 20 randomly selected dwarf individuals from the F_2 population to construct two bulks: a normal pool and a dwarf pool. Genomic DNA was isolated from fresh samples using the Plant Genomic DNA Kit (Tiangen, Beijing, China) following the manufacturer's instructions. The quality of genomic DNA was examined on a 1.5% agarose gel, and the purity was checked by a Nanodrop2000 spectrophotometer (Thermo Scientific, Wilmington, NC, USA). After quality control, two bulked DNA samples and two parent samples were selected for $30 \times$ resequencing. Then, the DNA fragments were subjected to purification, end-repair sequencing, and joint and PCR amplification and sequenced on the Illumina HiSeq 2500 platform. The filtered high-quality sequences were aligned and mapped to the Pumpkin

Genomics Database (<http://www.cucurbitgenomics.org/organism/9>) (accessed on 1 July 2022) using Burrows-Wheeler Aligner (BWA) for subsequent variation analysis [32]. SNPs and INDELS were detected using the mutation analysis software GATK [33]. According to a previous study, SNP-index and sliding-window analyses were performed [34].

2.4. Marker Development and Fine Mapping of the *CmaS11* Gene

According to the BSA-Seq results, KASP markers were designed based on target candidate region resequencing data for the two parents, and the KASP assay was performed following the protocol of LGC Genomics (Berlin, Germany), as reported previously [35]. An Applied Biosystems Viia 7 real-time PCR system (Applied Biosystems, Foster City, CA, USA) was used to detect allele-specific fluorescence, and all genotypes were called with Viia 7 software, v1.0. The KASP marker design strategy was as follows: 300–400 bp between each SNP, with SNPs preferentially located in coding regions. The primers used here are listed in Supplementary Table S1.

2.5. Candidate Gene Analysis

Based on the reference genome, the information in the mapping region of these genes was downloaded, including the gene ID, gene position, and functional annotation. These genes were first screened to determine whether they contributed to the dwarf phenotype. From the resequencing data of the two parents, we focused on key SNPs that caused stop-loss, stop-gain, or nonsynonymous mutations or splice-site variants as candidate SNPs. In addition, EMS mutations usually present as C-T or G-A SNPs. The primers used to amplify the genomic DNA or cDNA of the candidate genes were designed using Primer 5.0. The products of gene amplification were sequenced and aligned using DNAMAN software. The sequences of all polymorphic markers and primers used to amplify the candidate gene are listed in Table S1.

To analyze the sequence conservation for *GA3ox* across the amino acid sequences for Cucurbitaceae species, including cucumber, *C. maxima*, silver-seed gourd, wax gourd, bottle gourd, wild cucumber, and long cucumber, were downloaded from the Cucurbit Genomics Database. A neighbor-joining tree was generated with 1000 bootstrap replicates using MEGA 6.0. Quantitative real-time PCR (qRT-PCR) was carried out using a PrimeScript RT Reagent Kit (Tiangen, Beijing, China) in conjunction with QuantStudio 6 Flex (Life Technologies Corporation, Carlsbad, CA, USA) as described in the manufacturers' protocols. Three biological and three technical replicates were included for each experiment. The relative expression level of each gene was calculated using the $2^{-\Delta\Delta C_t}$ method [36] using the expression of *actin* as an internal control [37].

2.6. RNA-Sequencing and Data Analysis

The young stems containing wildtype and mutant internodes at the five-leaf and one-heart stages were harvested and stored at $-80\text{ }^{\circ}\text{C}$ for further analyses. Total RNA was extracted using an EasyPure Plant RNA Kit (Tiangen, Beijing, China), and the RNA purity was assessed utilizing an Agilent 2100 Bioanalyzer (Agilent Technologies, Palo Alto, CA, USA). All libraries were sequenced on an Illumina HiSeq 4000 platform (Illumina). Clean data were obtained by removing low-quality sequences, adaptor-contaminated sequences, and sequences with ambiguous base reads accounting for more than 5% of the raw data. The Hisat2 (<http://ccb.jhu.edu/software/hisat2/index.shtml>) (accessed on 1 July 2022) was used to align the clean reads with the Pumpkin Genomics Database (<http://www.cucurbitgenomics.org/organism/9>) (accessed on 1 July 2022). The fragments per kilobase per transcript per million mapped reads (FPKM) values were calculated and used to estimate the sequencing depth and gene length on the mapped read counts. Genes with an adjusted *p*-value (*padj*) < 0.05 and $|\log(\text{fold change})| \geq 1$ were assigned as differentially expressed. Gene Ontology (GO) terms and Kyoto Encyclopedia of Genes and Genomes (KEGG) pathways were enriched by differentially expressed genes (DEGs) if the *p* values were ≤ 0.05 .

2.7. Treatment with Exogenous GA_3

GA is known as a key plant hormone contributing to plant height, and exogenous GA treatment at different concentrations can restore dwarfing phenotypes. Based on the above result, candidate gene *CmoCh08G006170* is a key enzyme in the regulation of bioactive gibberellins (GAs). To determine whether dwarfing phenotypes of Si1 seedlings are related to gibberellin, exogenous GA treatment at different concentrations was conducted by spraying the Si1 seedlings. The germinated seeds were incubated in a greenhouse at 25.0 ± 1 °C with a 16 h/8 h light/dark cycle. At the two-leaf stage, the treated leaves were sprayed with 50 and 100 μM GA_3 , while the control seedlings were sprayed with water. Three biological replicates were sprayed three times every two days. The height from cotyledons to the growing point was measured 30 days after the final treatment.

3. Results

3.1. Distinct Phenotypes of the Dwarf Mutant

The dwarf mutant Si1 was much shorter than wildtype (WT) N87 (Figure 1A). The total length of the first twentieth node of Si1 (50.87 ± 0.88 cm) was reduced to 25.3% of that of the WT (200.68 ± 3.49 cm), and the eighth internode of Si1 (12.36 ± 0.40 cm) was reduced to 24.2% of that of the WT (50.94 ± 1.11 cm) (Table S2). These results showed that the length of the internodes of the dwarf mutant was approximately one-quarter of that of the WT, which could be visibly distinguished. However, there were no visible differences in leaf or stem diameter values (Figure 1B,C), which indicated that the mutant mainly changed the length of the main vine.

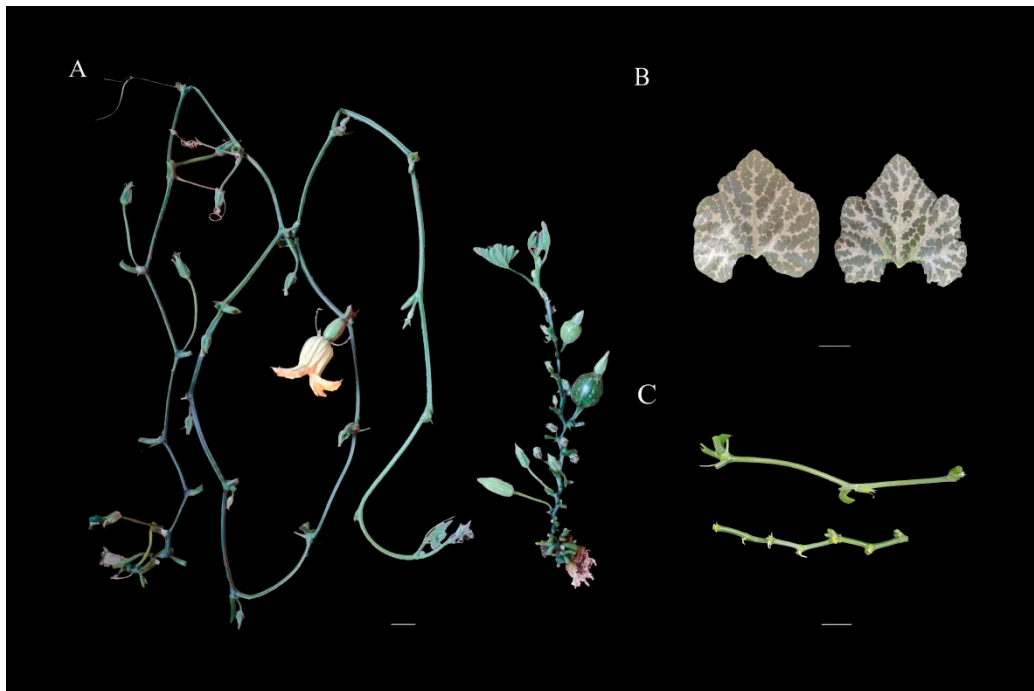


Figure 1. Morphological characterization of the two parental lines, Si1 and WT N87. (A), The whole-plant phenotypes of Si1 and WT N87. Bar, 5 cm. (B), Phenotype of a leaf of Si1 and WT N87. Bar, 2 cm. (C), Phenotype of the internodes of Si1 and WT N87. Bar, 2 cm.

To further analyze the cellular differences in the internodes of N87 and Si1, the cellular structure in the longitudinal section was observed and evaluated using optical microscopy (Figure 2A,B). From the microscopy images, the length of parenchyma cells in Si1 (72.9 ± 5.4 μm) was shorter than that in N87 (103.6 ± 8.3 μm), and the width of the cells in Si1 (63.2 ± 4.8 μm) was shorter than that in N87 (80.9 ± 6.7 μm), indicating that the mutant

had aberrant cell elongation (Figure 2C). Additionally, the number of parenchyma cells in Si1 ($64.5 \pm 8.4 \mu\text{m}$) was significantly increased compared with that in N87 ($42.1 \pm 5.8 \mu\text{m}$) (Figure 2D), suggesting that the reduced cell volume may be the main reason for the reduced internode length.

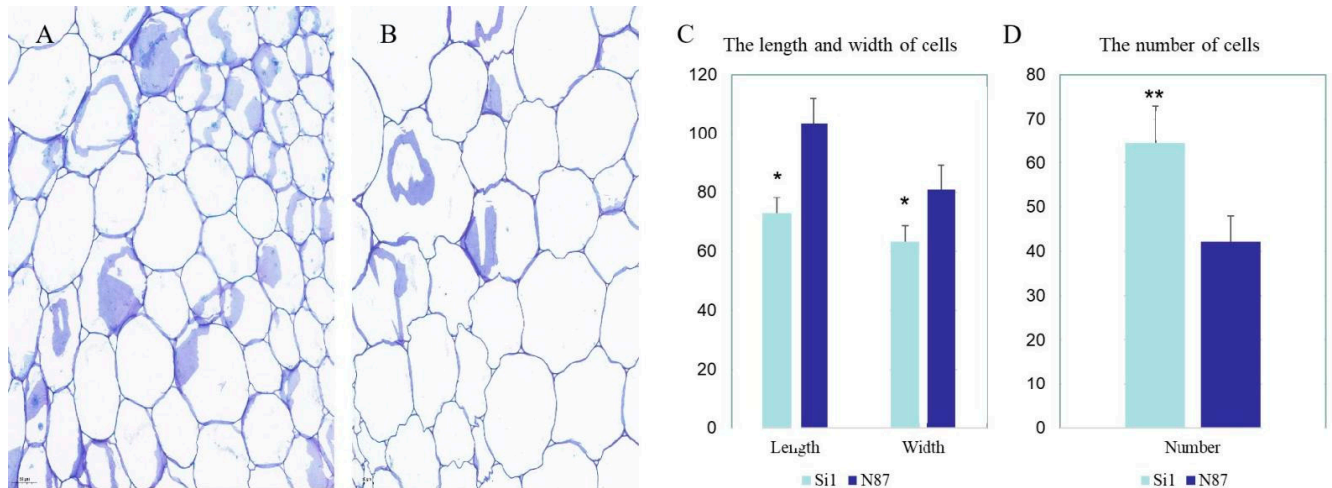


Figure 2. Cytological characterization of the parental lines Si1 and WT N87. (A,B), Longitudinal sections of the internodes of Si1 and WT N87. Bar, 50 μm . (C), The length and width of parenchyma cells in stems of Si1 and WT N87. (D), The number of cells in the Si1 and WT N87 longitudinal sections. Error bars indicate standard deviations from three repeats ($n = 3$). Values are means + SD ($n = 3$). ** Significant at $p < 0.01$, * Significant at $p < 0.05$.

3.2. Genetic Analysis of the Dwarf Mutant

To analyze the inheritance pattern of the dwarf mutant, Si1 was crossed with its original parent N87. The phenotype of all reciprocally crossed F_1 plants was normal; thus, the normal trait was dominant over the dwarf trait in the two lines. In the F_2 population, 56 of 244 individuals displayed the dwarf phenotype and 188 were normal, and the chi-square test confirmed this segregation ratio to be 3:1 ($\chi^2 = 0.55 < \chi^2_{0.05} = 3.84$). The BC_1P_1 population contained 80 individuals, with 80 normal individuals and no dwarf individuals. For BC_1P_2 , 61 individuals presented the dwarf phenotype while 63 individuals were normal, which fit a segregation ratio of 1:1 ($\chi^2 = 0.03 < \chi^2_{0.05} = 3.84$) (Table 1). These results indicate that the dwarf trait is controlled by a single recessive gene, which was named *CmaSI1*.

Table 1. Genetic analysis of the dwarf phenotype in *CmaSI1*.

Generations	No. Normal Individuals	No. Dwarf Individuals	No. Total Individuals	Expected Ratio	χ^2
$F_1 (P_1 \times P_2)$	40	0	40		
$F_1 (P_2 \times P_1)$	48	0	48		
$BC_1P_1 (F_1 \times N87)$	80	0	80		
$BC_1P_2 (F_1 \times Si1)$	63	61	124	1:1	0.03
$F_2 (1)$	188	56	244	3:1	0.55
$F_2 (2)$	1488	512	2000	3:1	0.38

3.3. Fine Mapping of the *CmaSI1* Locus by BSA-Seq and Linkage Analyses

Whole genome resequencing (WGR) through the BSA-Seq approach was used to identify the genomic region controlling the dwarf phenotype. A total of 273,422,085 raw reads were obtained from the dwarf pool ($21.62 \times$ average read depth with 93% coverage), and 273,422,085 raw reads were obtained from the normal pool ($24.23 \times$ average read depth with 93% coverage). In addition, the Q20 values (i.e., reads with average quality scores >20)

were all >90%, and the Q30 values (i.e., reads with average quality scores >30) were all >96%. These results indicate that the accuracy and quality of the sequencing data were sufficient for further analysis. To identify the genomic regions associated with dwarfism, the SNP index of each SNP locus was calculated between the two bulks using high-quality SNPs. The results revealed that there was only one candidate interval responsible for dwarfism; it was located in the 2,098,346–6,401,791 bp region on chromosome 8 (Figure 3A).

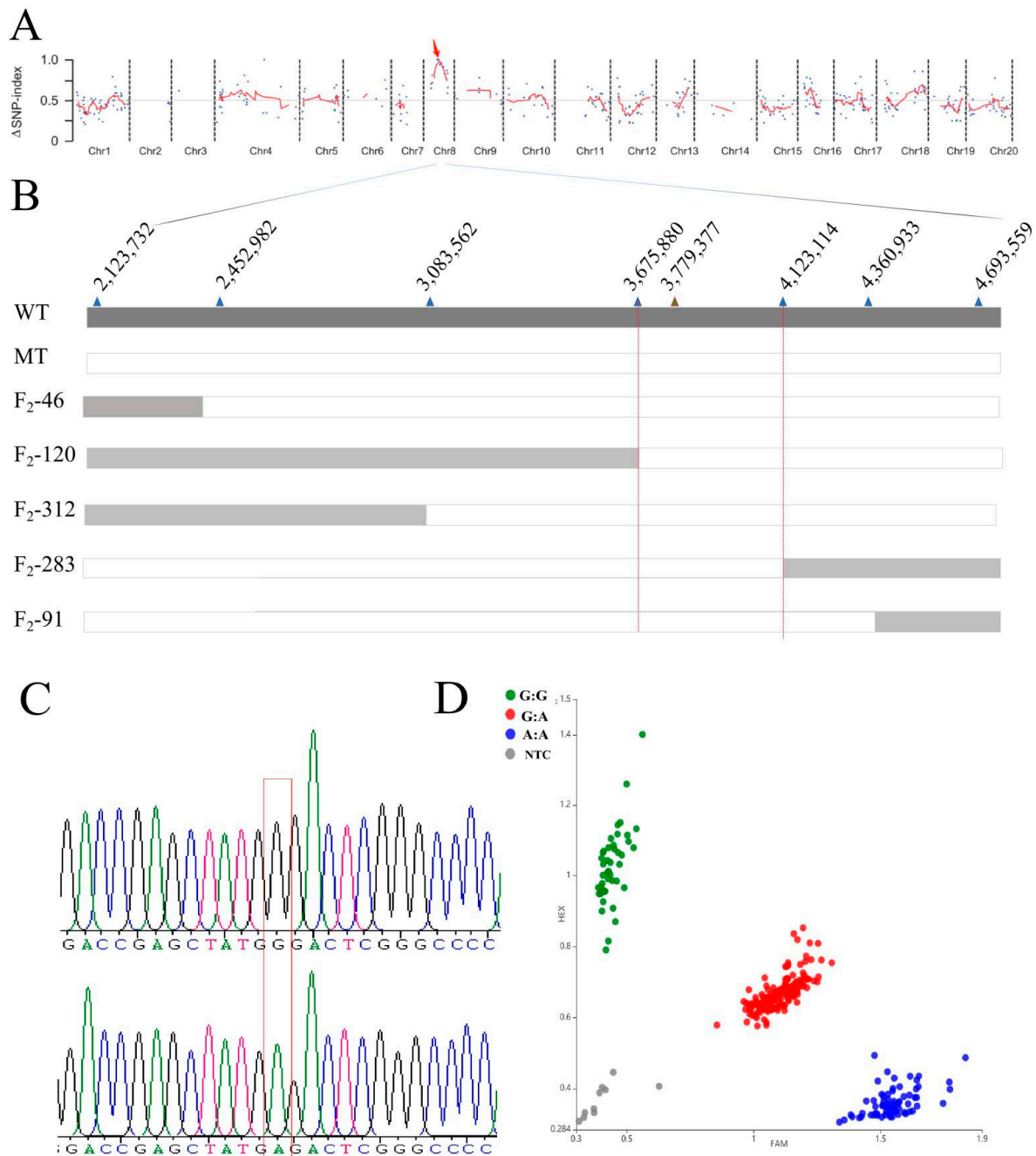


Figure 3. Mapping of the dwarfism gene *CmaS11*. (A), Delta SNP-index distribution on chromosome 8. (B), Fine mapping of *CmaS11*. The numbers within brackets indicate the number of recombinants. (C), The SNP found between the two parents on Chr08:3,779,377 was confirmed by sanger sequencing. (D), The corresponding KASP marker showed cosegregation in the F₂ population.

To further narrow the candidate region harboring the *CmaS11* locus, eight SNPs within the 4.4 Mb candidate region were designed as KASP markers and showed polymorphism

between the two parents. The marker information is shown in Table S1. Then, a total of 512 recessive individuals from the F₂ population were subsequently used for *CmaSI1* fine-mapping. Finally, the *CmaSI1* gene was mapped between SNP3675880 and SNP4123114, which each had one recombinant. The markers were physically located in a 463 kb region from 3,675,880 to 4,123,114 bp on chromosome 8 (Figure 3B).

3.4. Identification of Candidate Genes for the *CmaSI1* Gene

According to the fine mapping and the annotation information from the reference genome, 28 genes were predicted, and the physical positions and gene annotations of these genes are shown in Table S3. Among them, *CmoCh08G006140* encodes an auxin-responsive element, *CmoCh08G006170* encodes a gibberellin 3-beta hydroxylase and *CmoCh08G006180* encodes an ABC transporter protein [38,39]; all three of these may contribute to the dwarf phenotype. From the resequencing data of the two parents, we focused on seven SNPs that caused stop-loss, stop-gain, or nonsynonymous mutations or splice-site variants as candidate SNPs (Table 2). The seven SNPs were located on different genes, and only one SNP caused a nonsynonymous mutation (Chr08:3,779,377) in *CmoCh08G006170*. Furthermore, the SNP on *CmoCh08G006170* was confirmed by Sanger sequencing, and the corresponding KASP marker cosegregated in the F₂ population (Figure 3C,D). The mutation is a single nucleotide substitution from G to A that occurs in the second exon, leading to an amino acid substitution at codon 229 (Glu→Arg). *CmoCh08G006170* encodes a gibberellin 3-beta hydroxylase (*GA3ox*), which is a key enzyme in the regulation of bioactive GAs. Phylogenetic analysis indicated that the *CmoCh08G006170* gene has a close relationship with seventeen homologous genes and shares a common ancestor with *Carg23157* from a silver-seed gourd, suggesting that *Cla015407* was evolutionarily conserved within the Cucurbitaceae family (Figure 4B). Sequence analysis further revealed that *CmoCh08G006170* and its homologs are significantly conserved (Figure 4C). Nucleotide site 688 in *CmoCh08G006170* in all homologous genes presented a G encoding the highly conserved amino acid Glu. This result revealed that the SNP in the *CmoCh08G006170* gene may be the critical functional mutation.

Table 2. List of genes with SNPs.

Chromosome	Position	Gene_ID	WT	MT	Type
Cmo_Ch08	3688362	<i>CmoCh08G006070</i>	C	T	Intron
Cmo_Ch08	3747353	<i>CmoCh08G006150</i>	G	A	Intron
Cmo_Ch08	3779377	<i>CmoCh08G006170</i>	GGA:G	AGA:R	CDS_nonsyn
Cmo_Ch08	3815907	<i>CmoCh08G006250</i>	CTA:L	TTA:L	CDS_syn
Cmo_Ch08	3828051	<i>CmoCh08G006300</i>	G	A	Intron
Cmo_Ch08	4123114	<i>CmoCh08G006320</i>	G	A	Intron

3.5. Analysis of the Expression of GAs Biosynthetic Pathways and Regulatory Genes

To investigate the molecular mechanisms that underlie the Si1 dwarf, a comparative transcriptome analysis was used to identify DEGs between Si1 and WT. DEGs were screened based on set criteria (q value ≤ 0.05 and $|\log_2FC| > 1$), and totals of 976 DEGs (752 up-regulated and 224 down-regulated) were detected. For GO enrichment terms, DEGs were highly represented in the biological process category by the terms ‘oxidation reduction process’, ‘xyloglucan metabolic process’, and ‘negative regulation of peptidase activity’; in the cellular category, the most represented terms were cell periphery, ‘apoplast’ and ‘cell wall’. In addition, ‘oxidoreductase activity’, ‘oxidoreductase_activity’, and ‘oxidoreductase activity’ were among the most commonly represented molecular function terms. For KEGG pathways, the pathway ‘phenylpropanoid biosynthesis’ was the most common term, followed by ‘biosynthesis of secondary metabolites’, ‘metabolic pathways’, and ‘plant hormone signal transduction’ pathway.

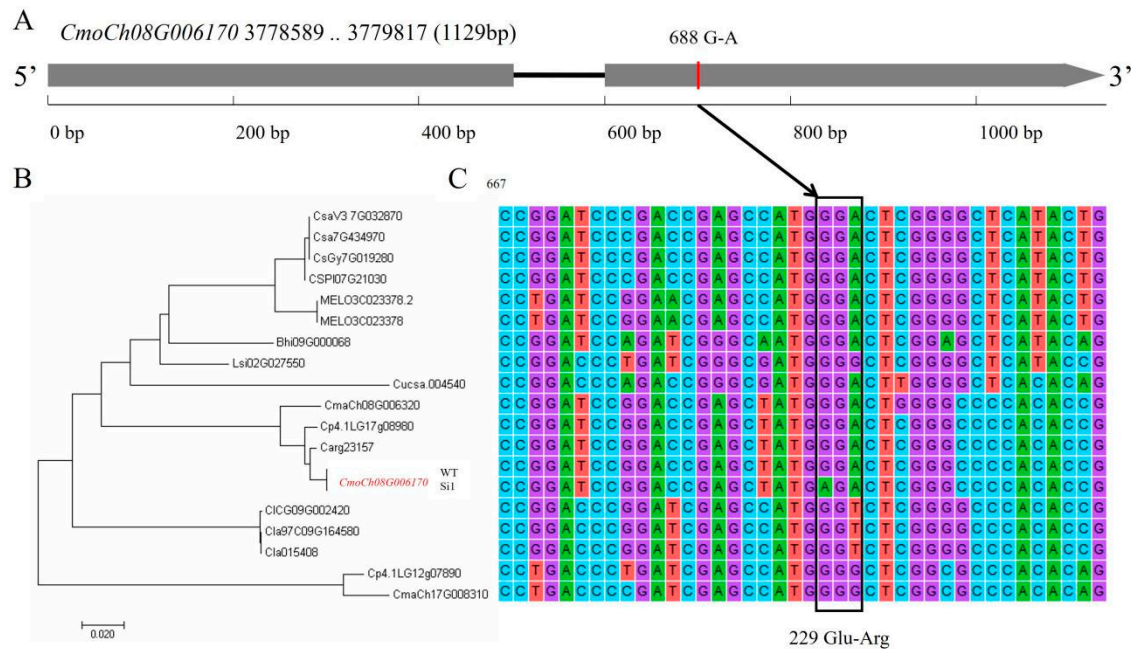


Figure 4. Gene structure, phylogenetic analysis, and sequence alignment of the *CmaSI1* gene in pumpkin. **(A)** The genomic structure of the predicted *CmaSI1* gene in pumpkin. The SNP presents a single nucleotide substitution from G to A that occurs in the second exon. **(B)** Phylogenetic analysis of *CmaSI1* proteins and their homologs in Cucurbitaceae species. **(C)** Sequence alignment of the *CmaSI1* gene and its homologs. Nucleotide site 688 in *CmoCh08G006170* in all homologous genes presented a G, resulting in the highly conserved amino acid Glu.

The synthesis of bioactive gibberellin is a complex process, and several DEGs that encode functional enzymes were well characterized from RNA-seq, including ent-copalyl diphosphate synthase (*CPS*), ent-kaurenoic acid oxidase (*KAO*), *GA20ox* and *GA3ox* (Figure 5). *GA20ox* (*CmoCh18G012300*, *CmoCh16G001660*, *CmoCh02G010360* and *CmoCh15G014590*) and *GA3ox* (*CmoCh08G006170*) were significantly up-regulated. Among them, *GA3ox* (*CmoCh08G006170*) was the candidate gene controlling the dwarf phenotype. Lester (1977) reported that *GA3ox* can be regulated by feedback and feedforward paths of active GAs, the low level of active GAs in vivo increases the transcription level of *GA3ox* [40]. We imply that a nonsynonymous mutation in *CmoCh08G006170* may influence its molecular function causing reduced active GAs. Furthermore, qRT-PCR results revealed that the expression level of *CmoCh08G006170* in stems of Si1 was significantly up-regulated compared with that in wild-type N87 (Figure 6). However, the expression of *CmoCh08G006170* in leaves and roots showed no difference between Si1 and N87. The result demonstrated the accuracy of the transcriptome analysis in the present study.

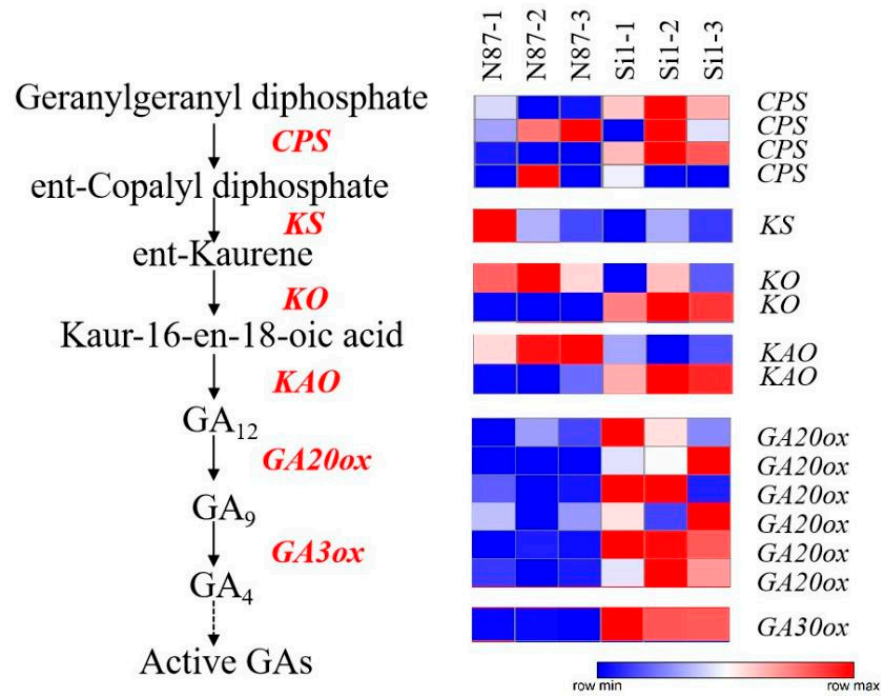


Figure 5. Analysis of the expression of GA biosynthetic related genes regulated by GAs.

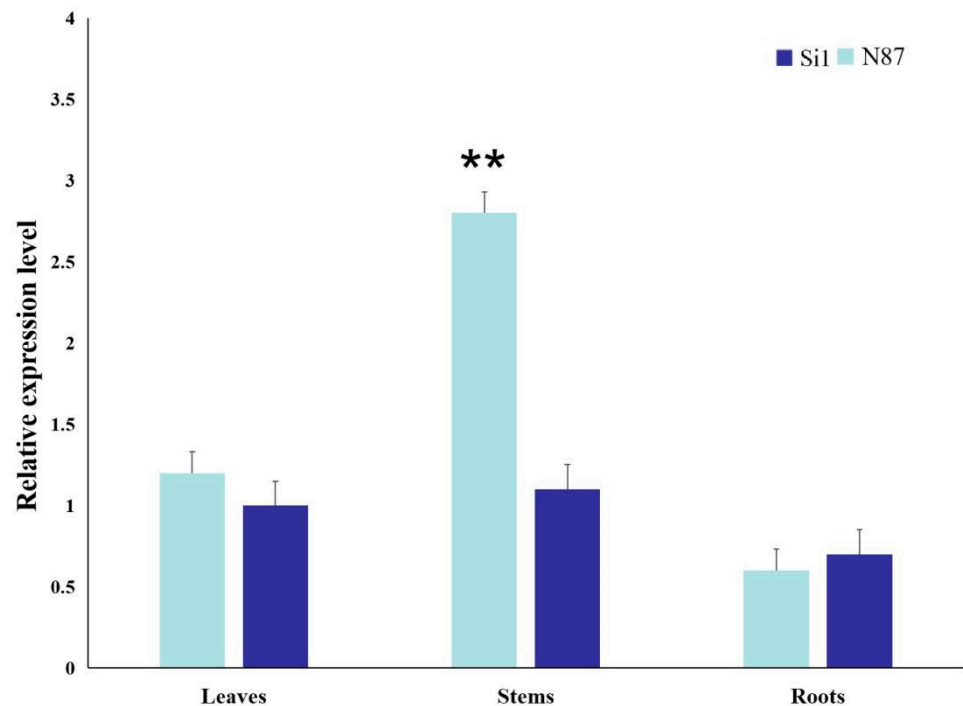


Figure 6. Relative expression level of *CmaSi1* in different tissues of Si1 and WT N87. Error bars indicate standard deviations from three repeats ($n = 3$). Values are means + SD ($n = 3$). ** Significant at $p < 0.01$.

3.6. *Si1* Is a GA Biosynthetic-Deficient Mutant

To test whether GAs regulate the height of the dwarf mutant, the mutant was treated with 50 and 100 μM GA_3 . After treatment with GA_3 solution, the lengths of the first eight main vines for WT, MT(H_2O) MT (100 μM GA_3) were 51.16 ± 1.16 cm, 12.19 ± 0.48 cm, and 50.77 ± 0.96 cm, and there was no significant difference between the wildtype and 100 μM GA_3 solution treatments (Figure 7). When the spraying concentration was 100 μM , the

vine length of Si1 and internode length were significantly restored, while spraying 50 μM GA_3 solution did not significantly increase the vine length or internode length. The results indicated that the dwarf phenotype is associated with decreased levels of bioactive GA_3 . Taken together, these results confirmed that Si1 is a GA biosynthetic-deficient mutant.

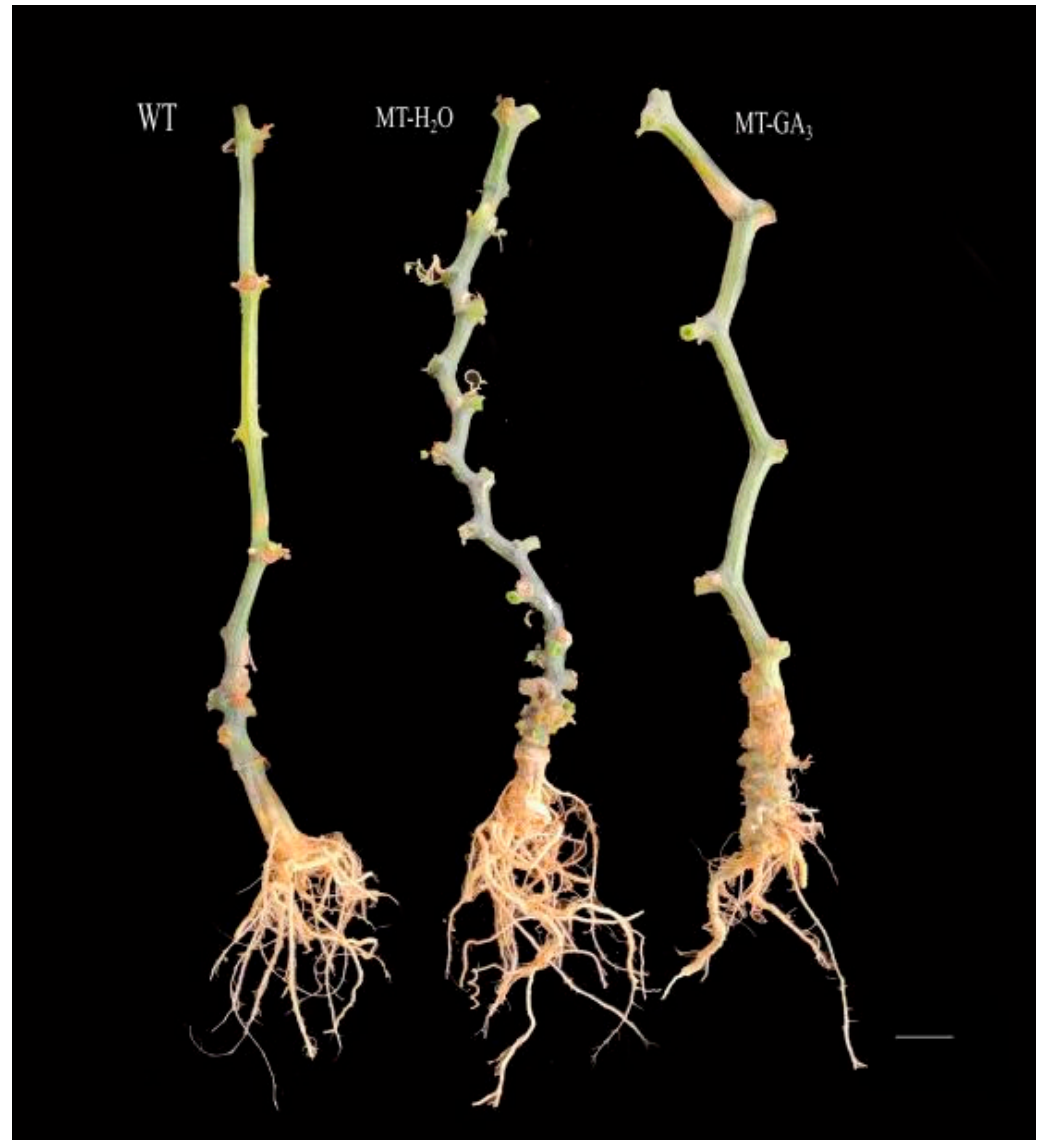


Figure 7. Recovery of the dwarf mutant by treatment with exogenous GA_3 . WT, mutant Si1 treated with 100 μM GA_3 , and mutant Si1 treated with H_2O are shown. Bar, 2 cm.

4. Discussion

Moderate dwarfing makes the plant type more compact and increases space utilization, which benefits rational dense planting and mechanized production. Many genes controlling dwarfing traits have been identified, and their molecular mechanisms have been analyzed. However, dwarfing traits often affect other agronomic traits, leading to clumps of plants, leaf shrinkage, and even reduced fertility, making it difficult to apply these traits in dwarfing breeding [41]. Therefore, it is particularly important to find and create dwarf germplasm resources with excellent characteristics. There are few studies on pumpkin dwarfing, and most of them have focused on *C. pepo* and *C. maxima*. Currently, the *C. moschata* dwarf lines bu and cga are clumping dwarfs with very short main vines, which have limited direct breeding value [29,42]. In this study, the dwarf mutant Si1 exhibited shortening of the main vine without changes to other traits, providing a new germplasm resource for the study

of dwarf *C. moschata* and resulting in the first *C. moschata* dwarf gene to be reported. In subsequent research, we will try to use this material for research on variety improvement.

EMS mutation technology and BSA technology have greatly improved the efficiency of new germplasm creation and gene function research. Ethyl methane sulfonate had a mutagenic effect, and since then, this method has been used in several different plants [17,43]. This method is widely used to induce mutants and construct mutant libraries because of its relatively low price, strong operability, and reusability. In our previous research, we successfully used mutation technology to construct a pumpkin mutant library that contains rich variation in traits related to leaves, plant type, reproductive organs, fruit, and other characteristics [31]. This library not only enriched the germplasm resources of *C. moschata* but also laid a foundation for the study of functional genomics and the breeding of new varieties of *C. moschata*. In addition, combined with BSA technology and fine mapping, we quickly used a small F₂ population to locate a target gene in a 463 kb region. Because EMS mutations usually present as C-T or G-A changes, the above types were screened from a large group of mutations found between the parents. Then, we focused on SNPs that caused stop-loss, stop-gain, or nonsynonymous mutations or splice-site variants to quickly identify candidate SNPs. In our study, only one predicted nonsynonymous mutation was found in the 463 kb mapping region; this mutation regulates bioactive GAs, which may contribute to the dwarf phenotype. At present, this strategy has also been successfully used in many studies to improve the efficiency of gene function research [17,44,45].

In this study, GA treatment rescued the dwarfing phenotype, suggesting that the dwarf-induced mutation was gibberellin-dependent, which confirmed that functional mutation of *GA3ox* causes GA-sensitive dwarf mutants. GA-sensitive mutants are often found in genes related to the GA biosynthesis pathway, and these mutations can lead to blockade of the GA biosynthesis pathway or the inability to synthesize bioactive GA. For these mutants, the dwarfing phenotype can be restored to the wildtype phenotype by spraying GA [46]. Currently, genes encoding enzymes related to GA biosynthesis or signal transduction pathways have been cloned [47,48]. In the GA biosynthesis pathway, CPS plays an early role in transforming geranylgeranyl diphosphate (GGDP) into CDP in plastids, and KAO in the endoplasmic reticulum catalyzes the conversion of ent-kaurene acid into *GA12* [49,50]. *GA3ox* and *GA20ox* play important roles in the final steps of the GA biosynthesis pathway [39,47]. *GA3oxs* transform *GA12* into bioactive GA and is a key gene in the last step of the GA synthesis pathway [41,47,48]. Four *GA3ox* homologs (*AtGA3ox1*, *AtGA3ox2*, *AtGA3ox3*, and *AtGA3ox4*) have been identified in *Arabidopsis thaliana* [51], with two *GA3ox* homologs in rice (*OsGA3ox1* and *OsGA3ox2*), and four *GA3ox* homologs in cucumber and pumpkin [52,53]. Several studies have confirmed functional changes in *GA3ox* mutations, such as *DWARF1* in maize, which can lead to dwarfism, a 13 bp deletion in a *GA3ox* gene causing a GA-deficient dwarf phenotype in watermelon, and mutations to two gibberellin 3-oxidase genes, *AtGA3ox1* and *AtGA3ox2*, that affect *Arabidopsis* development [18,51,54]. Our study showed that a single base mutation in *GA3ox* may influence its molecular function causing reduced active GAs. This study provides a new molecular basis for studying gibberellin-sensitive mutations.

5. Conclusions

We identified a dwarf mutant Si1 in pumpkin obtained by EMS mutagenesis of the inbred line N87. By BSA and subsequent fine mapping, we mapped the *CmaSI1* locus to a 463 kb region on chromosome 8 that contained 28 annotated genes in the F₂ population. Only one nonsynonymous SNP in *CmoCh08G006170* was obtained according to whole-genome resequencing of the two parents. *CmoCh08G006170*, a homolog of *Arabidopsis* gibberellin 3-beta hydroxylase (*GA3ox*), is a key enzyme in the regulation of bioactive gibberellins (GAs). RNA-seq analysis and qRT-PCR showed that the expression level of *CmoCh08G006170* in stems of Si1 was changed compared with that of wild type. The dwarf phenotype could be restored by exogenous GA₃ treatment, suggesting that Si1 is a

GA-deficient mutant. The above results demonstrated that *CmoCh08G006170* may be the candidate gene controlling the dwarf phenotype.

Supplementary Materials: The following supporting information can be downloaded at: <https://www.mdpi.com/article/10.3390/agronomy12081779/s1>, Table S1: List of primers in this study; Table S2: Morphological characterization of Si1 and WT N87; Table S3: Genes annotated in the mapping interval.

Author Contributions: Z.M. performed the experiments and wrote the manuscript. X.S. conceived the study and edited the manuscript. X.H. (Xinjun Hu), X.H. (Xiaoxia Han) and Y.L. analyzed the data and created the figures and tables. J.L., D.W. and L.S. coordinated the study. All authors have read and agreed to the published version of the manuscript.

Funding: This study was supported by grants from the National Natural Science Foundation of China-Youth Science Fund (32102408), the Natural Science Foundation of Hunan Province, China (2021JJ40300), the Science and Technology Innovation Program of Hunan Province, China (2021NK1006) and China Agriculture Research System of MOF and MARA (CARS-23-G-29).

Institutional Review Board Statement: Not applicable.

Informed Consent Statement: Not applicable.

Data Availability Statement: The data supporting the findings of this study are available within the article and its Supplementary Materials.

Acknowledgments: The work was performed at the Department of Horticulture, Hunan Agricultural University, Changsha, Hunan, 410128, China and Department of Vegetable Research Institute, Hunan Academy of Agricultural Sciences, Changsha, Hunan, 410125, China.

Conflicts of Interest: The authors declare no conflict of interest.

References

- Xiao, Z.; Fu, R.; Li, J.; Fan, Z.; Yin, H. Overexpression of the gibberellin 2-Oxidase gene from *Camellia lipoensis* induces dwarfism and smaller flowers in *Nicotiana tabacum*. *Plant Mol. Biol. Rep.* **2015**, *34*, 182–191. [[CrossRef](#)]
- Dong, W.; Wu, D.; Li, G.; Wu, D.; Wang, Z. Next-generation sequencing from bulked segregant analysis identifies a dwarfism gene in watermelon. *Sci. Rep.* **2018**, *8*, 2908. [[CrossRef](#)] [[PubMed](#)]
- Sasaki, A.; Ashikari, M.; Ueguchi-Tanaka, M.; Itoh, H.; Nishimura, A.; Swapan, D.; Ishiyama, K.; Saito, T.; Kobayashi, M.; Khush, G.S. Green revolution: A mutant gibberellin-synthesis gene in rice. *Nature* **2002**, *416*, 701–702. [[CrossRef](#)] [[PubMed](#)]
- Chai, S.; Yao, Q.; Zhang, X.; Xiao, X.; Wang, Y. The semi-dwarfing gene *Rht-dp* from dwarf Polish wheat (*Triticum polonicum* L.) is the “Green Revolution” gene *Rht-B1b*. *BMC Genom.* **2020**, *22*, 63. [[CrossRef](#)] [[PubMed](#)]
- Meland, M.; Frynes, O.; Maas, F. Performance of dwarfing and semi-dwarfing plum rootstocks on three European plum scion cultivars in a Nordic climate. *Acta Hort.* **2019**, *1260*, 181–186. [[CrossRef](#)]
- Velde, K.; Thomas, S.G.; Heyse, F.; Kaspar, R.; Rohde, A. N-terminal truncated RHT-1 proteins generated by translational reinitiation cause semi-dwarfing of wheat green revolution alleles. *Mol. Plant* **2021**, *14*, 9. [[CrossRef](#)] [[PubMed](#)]
- Bhuvanawari, S.; Krishnan, S.; Ellur, R.; Vinod, K.; Singh, A. Discovery of a novel induced polymorphism in *SD1* gene governing semi-dwarfism in rice and development of a functional marker for marker-assisted selection. *Plants* **2020**, *9*, 1198. [[CrossRef](#)]
- Monna, L.; Kitazawa, N.; Yoshino, R.; Suzuki, J.; Masuda, H.; Maehara, Y.; Tanji, M.; Sato, M.; Nasu, S.; Minobe, Y. Positional cloning of rice semi-dwarfing gene, *sd-1*: ‘Rice green revolution’ gene encodes a mutant enzyme involved in gibberellin synthesis. *DNA Res.* **2002**, *9*, 11–17. [[CrossRef](#)]
- Liu, C.; Zheng, S.; Gui, J.; Fu, C.; Yu, H.; Song, D.; Shen, J.; Qin, P.; Liu, X.; Han, B.; et al. Shortened basal internodes encodes a gibberellin 2-oxidase and contributes to lodging resistance in rice. *Mol. Plant* **2018**, *11*, 288–299. [[CrossRef](#)]
- Tang, T.; Acua, T.; Spielmeyer, W.; Richards, R. Effect of GA sensitive *rht18* and GA insensitive *rht-d1b* dwarfing genes on vegetative and reproductive growth in bread wheat. *J. Exp. Bot.* **2020**, *72*, 445–458. [[CrossRef](#)]
- Ford, B.; Foo, E.; Sharwood, R.; Karafiatova, M.; Vrana, J.; MacMillan, C.; Nichols, D.; Steuernagel, B.; Uauy, C.; Dolezel, J.; et al. *Rht18* semidwarfism in wheat is due to increased GA2-oxidaseA9 expression and reduced GA content. *Plant Physiol.* **2018**, *177*, 168–180. [[CrossRef](#)] [[PubMed](#)]
- Nakamura, A.; Fujioka, S.; Sunohara, H.; Kamiya, N.; Hong, Z.; Inukai, Y.; Miura, K.; Takatsuto, S.; Yoshida, S.; Ueguchi-Tanaka, M.; et al. The role of *OsBRI1* and its homologous genes, *OsBRL1* and *OsBRL3*, in rice. *Plant Physiol.* **2006**, *140*, 580–590. [[CrossRef](#)]
- Multani, D.; Briggs, S.; Chamberlin, M.; Blakeslee, J.; Murphy, A.; Johal, G. Loss of an MDR transporter in compact stalks of maize *br2* and sorghum *dw3* mutants. *Science* **2003**, *302*, 81–84. [[CrossRef](#)] [[PubMed](#)]

14. Tamiru, M.; Undan, J.; Takagi, H.; Abe, A.; Yoshida, K.; Undan, J.; Satoshi, N.; Aiko, U.; Hiromasa, S.; Hideo, M.; et al. A cytochrome P450, *OsDSS1*, is involved in growth and drought stress responses in rice (*Oryza sativa* L.). *Plant Mol. Biol.* **2015**, *88*, 85–99. [[CrossRef](#)] [[PubMed](#)]
15. Zhu, H.; Zhang, M.; Sun, S.; Yang, S.; Yang, L. A single nucleotide deletion in an ABC transporter gene leads to a dwarf phenotype in watermelon. *Front. Plant Sci.* **2019**, *10*, 1399. [[CrossRef](#)]
16. Hong, Z.; Ueguchi-Tanaka, M.; Matsuoka, M. Brassinosteroids and rice architecture. *J. Pestic. Sci.* **2004**, *29*, 184–188. [[CrossRef](#)]
17. Yang, B.; Zhou, S.; Ou, L.; Liu, F.; Yang, L.; Zheng, J.; Chen, W.; Zhang, Z.; Yang, S.; Ma, Y.; et al. A novel single-base mutation in *CaBRI1* confers dwarf phenotype and brassinosteroid accumulation in pepper. *Mol. Genet. Genom.* **2020**, *295*, 343–356. [[CrossRef](#)] [[PubMed](#)]
18. Wei, C.; Zhu, C.; Yang, L.; Zhao, W.; Ma, R.; Li, H.; Zhang, Y.; Ma, J.; Yang, J.; Zhang, X. A point mutation resulting in a 13 bp deletion in the coding sequence of *Cldf* leads to a GA-deficient dwarf phenotype in watermelon. *Hortic. Res.* **2019**, *6*, 132. [[CrossRef](#)] [[PubMed](#)]
19. Lin, T.; Wang, S.; Zhong, Y.; Gao, D.; Cui, Q.; Chen, H. A truncated F-box protein confers the dwarfism in cucumber. *J. Genet. Genom.* **2016**, *43*, 223–226. [[CrossRef](#)] [[PubMed](#)]
20. Xu, L.; Chao, W.; Wen, C.; Zhou, S.; Tao, W. *Clavata1*-type receptor-like kinase *csclavata1* is a putative candidate gene for dwarf mutation in cucumber. *Mol. Genet. Genom.* **2018**, *293*, 1393–1405. [[CrossRef](#)]
21. Huang, S.; Li, R.; Zhang, Z.; Li, L.; Gu, X.; Fan, W.; Lucas, W. The genome of the cucumber, *Cucumis sativus* L. *Nat. Genet.* **2009**, *41*, 1275–1281. [[CrossRef](#)] [[PubMed](#)]
22. Li, Y.; Yang, L.; Pathak, M.; Li, D.; He, X.; Weng, Y. Fine genetic mapping of *cp*: A recessive gene for compact (dwarf) plant architecture in cucumber, *Cucumis sativus* L. *Theor. Appl. Genet.* **2011**, *123*, 973. [[CrossRef](#)] [[PubMed](#)]
23. Zhang, F.; Jiang, Z.; Zhang, E. Pumpkin function properties and application in food industry. *Sci. Technol. Food Ind.* **2000**, *2*, 62–64.
24. Yadav, M.; Jain, S.; Tomar, R.; Prasad, G.; Yadav, H. Medicinal and biological potential of pumpkin: An updated review. *Nutr. Res. Rev.* **2010**, *23*, 184–190. [[CrossRef](#)] [[PubMed](#)]
25. Jun-Xin, W.; Chang, Z. A construction of aflp analysis system for dwarf *Cucurbita moschata* research. *Acta Agric. Boreali-Sin.* **2011**, *26*, 124–127.
26. Xiang, C.; Duan, Y.; Li, H.; Ma, W.; Huang, S.; Sui, X.; Zhang, Z.; Wang, C. A high-density EST-SSR-based genetic map and QTL analysis of dwarf trait in *Cucurbita pepo* L. *Int. J. Mol.* **2018**, *19*, 3140. [[CrossRef](#)]
27. Wang, R.; Huang, H.; Lin, Y.E.; Chen, Q.; Liang, Z.; Wu, T. Genetic and gene expression analysis of *dm1*, a dwarf mutant from *Cucurbita maxima* Duch. ex Lam, based on the AFLP method. *Can. J. Plant Sci.* **2014**, *94*, 293–302. [[CrossRef](#)]
28. Zhang, G.; Ren, Y.; Sun, H. A high-density genetic map for anchoring genome sequences and identifying QTLs associated with dwarf vine in pumpkin (*Cucurbita maxima* Duch.). *BMC Genom.* **2015**, *16*, 1101–1110. [[CrossRef](#)]
29. Wu, T.; Cao, J. Differential gene expression of tropical pumpkin (*Cucurbita moschata* Duchesne) bush mutant during internode development. *Sci. Hortic.* **2008**, *117*, 219–224. [[CrossRef](#)]
30. Min, Z.; Han, X.; Li, Y.; Hu, X.; Wang, D.; Sun, X. Construction and preliminary screening of EMS induced mutant library of pumpkin (*Cucurbita moschata* D.). *J. Nucl. Agr. Sci.* **2021**, *35*, 761–768.
31. Hu, X.; Su, J.; Yuan, Z.; Li, Y.; Han, X. Breeding of xingshudaguomiben, a pumpkin cultivar with high yield and high quality. *J. Chang. Veg.* **2015**, *12*, 6–7.
32. Li, H.; Durbin, R. Fast and accurate short read alignment with Burrows–Wheeler transform. *Bioinformatics* **2009**, *25*, 1754–1760. [[CrossRef](#)] [[PubMed](#)]
33. McKenna, A.; Hanna, M.; Banks, E.; Sivachenko, A.; Cibulskis, K.; Kernysky, A.; Garimella, K.; Altshuler, D.; Gabriel, S.; Daly, M.; et al. The Genome Analysis Toolkit: A MapReduce framework for analyzing next-generation DNA sequencing data. *Genome Res.* **2010**, *20*, 1297–1303. [[CrossRef](#)]
34. Song, J.; Li, Z.; Liu, Z.; Guo, Y.; Qiu, L. Next-generation sequencing from bulked-segregant analysis accelerates the simultaneous identification of two qualitative genes in soybean. *Front. Plant Sci.* **2017**, *8*, 919. [[CrossRef](#)] [[PubMed](#)]
35. Rasheed, A.; He, Z.; Gao, F.; Zhai, S.; Jin, H.; Liu, J.; Guo, Q.; Zhang, Y.; Dreisigacker, S.; Xia, X.; et al. Development and validation of KASP assays for genes underpinning key economic traits in bread wheat. *Theor. Appl. Genet.* **2016**, *129*, 1843–1860. [[CrossRef](#)]
36. Livak, K.; Schmittgen, T. Analysis of relative gene expression data using real-time quantitative PCR and the $2^{-\Delta\Delta CT}$ method. *Methods* **2001**, *25*, 402–408. [[CrossRef](#)]
37. Ding, W.; Wang, Y.; Qi, C.; Luo, Y.; Qu, S. Fine mapping identified the gibberellin 2-oxidase gene *cpdw* leading to a dwarf phenotype in squash (*Cucurbita pepo* L.). *Plant Sci.* **2021**, *306*, 110857. [[CrossRef](#)]
38. Ling-Duo, B.; Si-Gui, J.; Jiang-Zhou, L. The effects of gibberellin (GA_3) concentration on the growth, yield and quality of tobacco upper leaves. *J. Anhui Agric. Sci.* **2018**, *46*, 46–51.
39. Hwang, J.; Song, W.; Hong, D.; Ko, D.; Yamaoka, Y.; Jang, S. Plant ABC transporters enable many unique aspects of a terrestrial plant's lifestyle. *Mol. Plant* **2016**, *9*, 18. [[CrossRef](#)] [[PubMed](#)]
40. Lester, D.; Ross, J.; Davies, P.; Reid, J. Mendel's stem length gene (*Le*) encodes a gibberellin 3β -hydroxylase. *Plant Cell* **1997**, *9*, 1435–1443.
41. Wang, Y.; Zhao, J.; Lu, W.; Deng, D. Gibberellin in plant height control: Old player, new story. *Plant Cell Rep.* **2017**, *36*, 391–398. [[CrossRef](#)] [[PubMed](#)]

42. Wu, T.; Cao, J.; Qin, Z.; Du, Y. Identification of a novel GA-related bush mutant in pumpkin (*Cucurbita moschata* Duchesne). *Pak. J. Bot.* **2015**, *47*, 1359–1366.
43. Wang, D.; Wang, S.; Chao, J.; Wu, X.; Sun, Y.; Li, F.; Gao, X.; Liu, G.; Wang, Y. Morphological phenotyping and genetic analyses of a new chemical-mutagenized population of tobacco (*Nicotiana tabacum* L.). *Planta* **2017**, *246*, 149–163. [[CrossRef](#)]
44. Hao, N.; Du, Y.; Li, H.; Wang, C.; Wang, C.; Gong, S. *Csmyb36* is involved in the formation of yellow green peel in cucumber (*Cucumis sativus* L.). *Theor. Appl. Genet.* **2018**, *131*, 1659–1669. [[CrossRef](#)]
45. Li, X.; Xiang, F.; Zhang, W.; Yan, J.; Li, X.; Zhong, M.; Yang, P.; Chen, C.; Liu, X.; Mao, D.; et al. Characterization and fine mapping of a new dwarf mutant in *Brassica napus*. *BMC Plant Biol.* **2021**, *21*, 117. [[CrossRef](#)]
46. Ashikari, M.; Itoh, H.; Miyako, U. Gibberellin in signal transduction in rice. *Plant Growth Regul.* **2003**, *22*, 141–151. [[CrossRef](#)]
47. Sun, T. The molecular mechanism and evolution of the GA-GID1-DELLA signaling module in plants. *Curr. Biol.* **2011**, *21*, 338–345. [[CrossRef](#)]
48. Binenbaum, J.; Weinstain, R.; Shani, E.; Kamiya, Y. Gibberellin localization and transport in plants. *Trends Plant Sci.* **2018**, *23*, 410–421. [[CrossRef](#)]
49. Yamaguchi, S.; Sun, T.; Kawaide, H.; Kamiya, Y. The GA₂ locus of *Arabidopsis thaliana* encodes *ent*-kaurene synthase of gibberellin biosynthesis. *Plant Physiol.* **1998**, *116*, 1271–1278. [[CrossRef](#)]
50. Wu, Z.; Tang, D.; Liu, K.; Miao, C.; Zhuo, X.; Li, Y.; Tan, X.; Sun, M.; Luo, Q.; Cheng, Z. Characterization of a new semi-dominant dwarf allele of *SLR1* and its potential application in hybrid rice breeding. *J. Exp. Bot.* **2018**, *69*, 4703–4713. [[CrossRef](#)]
51. Mitchum, M.; Yamaguchi, S.; Hanada, A.; Kuwahara, A.; Yoshioka, Y.; Kato, T.; Tabata, S.; Kamiya, Y.; Sun, T. Distinct and overlapping roles of two gibberellin 3-oxidases in *Arabidopsis* development. *Plant J.* **2006**, *45*, 804–818. [[CrossRef](#)] [[PubMed](#)]
52. Pimenta, L.; Knop, N.; Theo, L. Stamen-derived bioactive gibberellin is essential for male flower development of *Cucurbita maxima* L. *J. Exp. Bot.* **2012**, *63*, 2681–2691. [[CrossRef](#)] [[PubMed](#)]
53. Pimenta, L.; Liebrandt, A.; Arnold, L.; Chmielewska, S.; Felsberger, A.; Freier, E.; Heuer, M.; Zur, D.; Lange, T. Functional characterization of gibberellin oxidases from cucumber, *Cucumis sativus* L. *Phytochemistry* **2013**, *90*, 62–69. [[CrossRef](#)]
54. Chen, Y.; Hou, M.; Liu, L.; Wu, S.; Shen, Y.; Ishiyama, K.; Kobayashi, M.; McCarty, D.; Tan, B. The maize *DWARF1* encodes a gibberellin 3-oxidase and is dual localized to the nucleus and cytosol. *Plant Physiol.* **2014**, *166*, 2028. [[CrossRef](#)]